

# Rigidity and intermediate phases in glasses driven by speciation

Matthieu Micoulaut

Laboratoire de Physique Théorique de la Matière Condensée,  
Université Pierre et Marie Curie, Boite 121  
4, Place Jussieu, 75252 Paris Cedex 05, France

(Dated: January 27, 2020)

The rigid to floppy transitions and the associated intermediate phase in glasses are studied in the case where the local structure is not fully determined from the macroscopic concentration. The approach uses size increasing cluster approximations and constraint counting algorithms. It is shown that the location and the width of the intermediate phase and the corresponding structural, mechanical and energetical properties of the network depend crucially on the way local structures are selected at a given concentration. The broadening of the intermediate phase is obtained for networks combining a large amount of flexible local structural units and a high rate of medium range order.

PACS numbers: 61.43.Fs-61.20.-x

Concepts from mean-field rigidity in networks found their origin from Lagrangian constraint counting in mechanics [1] and have been applied with great success in glass science for several decades [2]. Bonds in a glass network can indeed be considered as constraints arising from interatomic stretching and bending forces. The connectivity or cross-link density (best quantified by the network mean coordination number  $\bar{r}$ ) plays therefore a key role. In highly cross-linked networks where  $\bar{r}$  is large, there are more constraints than degrees of freedom per atom on average and the structure is stressed rigid (hyperstatic or overconstrained). At low connectivity, one has a flexible (hypostatic or underconstrained) structure that contains more degrees of freedom than constraints. Thorpe [3] analyzed the vibrational behaviour of such kind of networks and identified a mean-field (MF) floppy to rigid transition when the mean coordination number equals  $\bar{r} = \bar{r}_c = 2.38$ , a result that agrees with global (Maxwell) constraint counting as enunciated by Phillips [4] from the enumeration  $n_c$  of bond stretching and bond bending forces.

The underlying nature of this peculiar transition has been deeply reinvestigated recently because two transitions at  $\bar{r}_{c(1)}$  and  $\bar{r}_{c(2)}$  have been found [5] experimentally in a variety of glasses. These define an intervening region (or intermediate phase, (IP)) between the floppy and the stressed rigid phase. In the IP, glasses display some remarkable properties such as absence of ageing [6] or stress [7], selection of isostatically rigid local structures [5] or weak birefringence [8]. The two boundaries have been characterized from numerical calculations [9] and cluster analysis [10] on self-organized networks and identified as being a rigidity transition at low  $\bar{r}$  and a stress transition at high  $\bar{r}$ . In the mean-field approach or in random networks where self-organization does not take place, both transitions coalesce into a single one. Moreover, links between IP and protein folding [11], high-temperature superconductors [12] or computational

phase transitions [13] have been stressed that go much beyond simple analogies. The understanding of the IP is therefore of general interest. It has become clear that stress avoidance in the network is responsible for the width  $\Delta\bar{r} = \bar{r}_{c(2)} - \bar{r}_{c(1)}$  and the location of the intermediate phase, an idea that has gained some strength from energetical adaptation in a simple random bond model [14] for the rigidity transition or suppressed nucleation of rigidity during a fluid-solid transition [15]. Mousseau and co-workers [16] have also shown recently that self-organization with equilibration on diluted triangular lattices would lead to an intermediate phase.

However, the recent discovery of an IP in more complex glass systems such as silicates [17] raises a new challenging issue. On the experimental side, most of the results have been obtained up to now on simple network glasses (e.g. the archetypal  $Ge_xSe_{1-x}$ ), where  $\bar{r}$  can be directly related to the concentration ( $\bar{r} = 2 + 2x$ ) of the species involved [18]. This happens to be not the case any more in multicomponent systems such as (even simple) binary glasses (a network former, e.g.  $SiO_2$  and a modifier, e.g.  $Li_2O$ ) where a non-trivial speciation can appear depending on the nature of the cation or the atoms involved. This contributes to  $\bar{r}$  in a non-linear fashion and application of constraint counting algorithms becomes more difficult. We describe in this Letter how speciation affects onset of rigidity and the intermediate phase. A simple model to highlight the effect of the speciation is solved, and combined with cluster-constraint calculations applied to silicate or thiosilicates of the form  $(1-x)SiX_2 - xM_2X$  with ( $X = O, S, Se$ ) and ( $M = Li, Na, K$ ) which are known [19] to display a mean-field rigidity transition at  $x = 0.20$ . The presence of an intermediate phase is demonstrated and its structural, mechanical and energetical properties characterized. It appears that the selection of more flexible local structural units with addition of a modifier leads to a broadening of the IP, independently of the degree

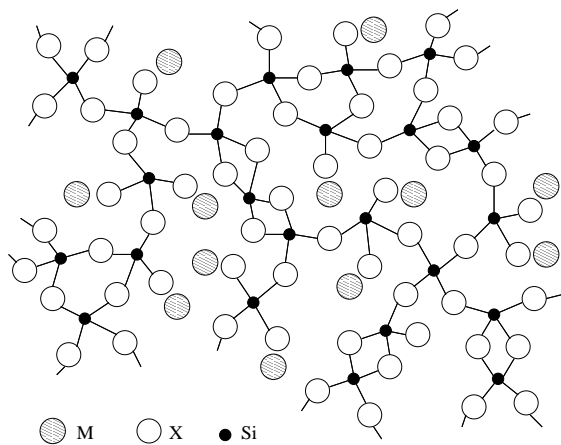


FIG. 1: An example of a network made of 23 tetrahedra with 4  $Q^2$ , 4  $Q^3$  and 15  $Q^4$  units, corresponding to the modifier concentration  $x = 0.207$ . The fraction of edge-sharing tetrahedra is  $\eta = 0.32$ .

of medium range order. The latter contributes however to the increase of  $\Delta\bar{r}$  as well. On the other hand, the possibility of the system to adapt the speciation in order to lower the constraint free energy in the stressed rigid phase leads to a situation that resembles very much to sodium silicates. Taken together, these results provide new benchmarks to study IP's in multicomponent oxide or chalcogenide glass systems such as fast ionic amorphous superconductors where the speciation and henceforth the elastic nature of the network crucially determine physical and electric transport properties.

In binary sodium silicates ( $X=O$ ,  $M=Na$ ), speciation depends weakly [20] on the nature of the modifier cation  $M$  which creates almost only  $Q^{n=3}$  units at low  $x$  so that the probability of finding the latter is  $R = 2x/(1-x)$ . Here, the superscript " $n = 3$ " denotes the number of bridging oxygens on a  $SiO_{4-n/2}M_{4-n}$  tetrahedron (a  $Q^n$  unit) that connects to the rest of the network (Fig. 1). This means that the chemical reaction [21]:



involving the species  $Q^n$  is disequibrated on the left side. A radically different situation is encountered in systems with modifier cations of smaller sizes ( $M=Li$ ) or in thiosilicates ( $X=S$ ) and selenosilicates ( $X=Se$ ) [22]. Certain of these glass networks can be indeed made out of  $Q^4$  and  $Q^2$  species only or, at least, of a mixture of all  $Q^n$ 's. Noteworthy is the fact that Maxwell constraint counting [4] does not distinguish between the aforementioned systems, although the location of the rigidity and stress transitions should be obviously changed.

Size increasing cluster approximations (SICA) can be used [10] to infer the effect of speciation on the location and the width of the intermediate phase. We consider a network of  $N$  tetrahedra  $Q^4$ ,  $Q^3$  and  $Q^2$  (see

Fig. 1) with respective probabilities  $p_4^{(1)}$ ,  $p_3^{(1)}$  and  $p_2^{(1)}$ . The behaviour of the  $p_i^{(1)}$ 's with modifier concentration  $x$  can be determined from the normalization condition  $p_4^{(1)} + p_3^{(1)} + p_2^{(1)} = 1$ , the charge conservation law [23]  $R = p_3^{(1)} + 2p_2^{(1)}$ , and finally the definition of the equilibrium constant [24] of the chemical reaction (1) given by:  $K_e = p_4^{(1)} p_2^{(1)} / p_3^{(1)} p_3^{(1)}$ . For instance, in lithium silicates [25]  $K_e$  is of the order of 0.3 at  $x = 0.17$ . With these equations, the speciation is fully determined with respect to  $x$  and given by:

$$p_3^{(1)} = \frac{R(2-R)}{1 + \sqrt{(1-R)^2 + 4K_e R(2-R)}} \quad (2)$$

out of which is obtained  $p_2^{(1)} = (R - p_3^{(1)})/2$  and  $p_4^{(1)} = 1 - p_3^{(1)} - p_2^{(1)}$ . Starting from this short-range order distribution  $p_i^{(1)}$  (the basic SICA units at the initial step  $l = 1$  which will serve as building blocks), one constructs the 12 possible structural arrangements of two basic units ( $l = 2$ ), i.e.  $Q^4 - Q^4$ ,  $Q^4 - Q^3$ ,  $Q^4 - Q^2$ ,  $Q^3 - Q^3$ , etc. Three energy gains,  $E_{stress}$ ,  $E_{iso}$  and  $E_{flex}$  with corresponding Boltzmann factors  $e_i = \exp[-E_i/k_B T]$ , are defined following the mechanical nature of the created cluster (stressed rigid, isostatically rigid and flexible). The probabilities of the created clusters ( $l = 2$ ) are then given by  $p_{kj}^{(2)} \propto W_{kj} p_k^{(1)} p_j^{(1)} e_i$  ( $i = stress, iso, flex$ ) where  $W_{kj}$  is a statistical factor taking into account the number of equivalent ways to connect two ( $l = 1$ ) units together. For instance, there are  $W_{44} = 72$  different ways to connect two  $Q^4$  tetrahedra by edges. One should also note that there are only two stressed rigid clusters created (corner and edge-sharing  $Q^4 - Q^4$  connections) and one isostatically rigid cluster ( $n_c = 3.0$ , a corner-sharing  $Q^4 - Q^3$  connection). Maxwell constraint counting [3] is then applied on the set of ( $l = 2$ ) clusters that leads to the number of floppy modes of the network given by:

$$f^{(2)} = 3 - n_c^{(2)} = 3 - \frac{\sum_{k,j} n_c(kj) p_{kj}^{(2)}}{\sum_{k,j} N_{kj} p_{kj}^{(2)}} \quad (3)$$

where  $n_c(kj)$  and  $N_{kj}$  are respectively the number of mechanical constraints and the number of atoms of the cluster with probability  $p_{kj}^{(2)}$ . Once this is set and starting from a flexible (floppy) network where stressed rigid dendritic  $Q^4 - Q^4$  connections are absent and decreasing  $x$ , one can investigate at which concentration  $x_{c(1)}$  the network will have a vanishing of  $f^{(2)}$  (rigidity transition) and at which concentration  $x_{c(2)}$  the network will not be able to avoid stressed rigid dendritic clusters (i.e. corner-sharing  $Q^4$ ) any more (stress transition). These corner-sharing  $Q^4$ 's contribute to percolation of stressed rigidity. The calculation is performed for a given amount of medium range order characterized by the fraction  $\eta$  of edge-sharing tetrahedra in the base glass ( $x = 0$ ). This furthermore suggests that the strain can be concentrated in small rings and structures.

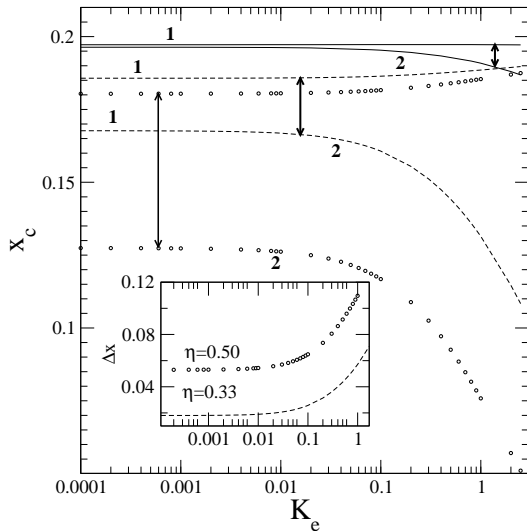


FIG. 2: Location of the rigidity (label 1) and the stress transition (label 2) as a function of the equilibrium constant  $K_e$  for three fractions of edge-sharing tetrahedra in the base glass  $\eta = 0.04$  (solid line),  $\eta = 0.33$  (broken line) and  $\eta = 0.50$  (dots). Vertical arrows serve to identify the width  $\Delta x$  of the intermediate phase at a given  $K_e$ . The insert shows the corresponding width of the intermediate phase.

Fig. 2 shows the results of the construction. Large equilibrium constant  $K_e$  (corresponding to a  $Q^2$ -rich glass) will induce a large width for the IP. However, one observes that  $K_e$  mostly affects the location  $x_{c(2)}$  of the stress transition whereas the location of the rigidity transition  $x_{c(1)}$  remains almost constant, as already signaled [10] for a network glass. Noteworthy is also the shift from the MF rigidity transition at  $x_c = 0.20$  to lower  $x$  that arises from the presence of weakly stressed rigid edge-sharing tetrahedra (EST,  $n_c = 3.33$  per atom). With a weaker rigidity due to the presence of these EST, part of the strain is captured in the EST, and onset of flexibility can happen at lower modifier concentration  $x$ . As for IV-VI network glasses [10], the width  $\Delta x = x_{c(2)} - x_{c(1)}$  of the IP increases with the fraction  $\eta$  of EST due to the shift of the location of the stress transition (Fig. 2). The change in speciation from a  $Q^3$ -rich to a  $Q^2$ -rich glass contributes however to an additional broadening of the IP. The trend with  $K_e$  observed in Fig. 2 can be further characterized from the computation of the probability of stressed rigid and isostatically rigid clusters using SICA. When the chemical reaction (1) is desequilibrated on the left side (low  $K_e$ , i.e. a  $Q^3$ -rich glass), each modifier molecule will create mostly two flexible  $Q^3$  units ( $n_c = 2.55$  per atom) that serve to accumulate isostatically rigid subregions of the network, as  $Q^4 - Q^3$  connections are likely to appear. These are maximum at the stress transition (solid line, Fig. 3), consistently with numerical simulations [9]. On the other hand, a higher

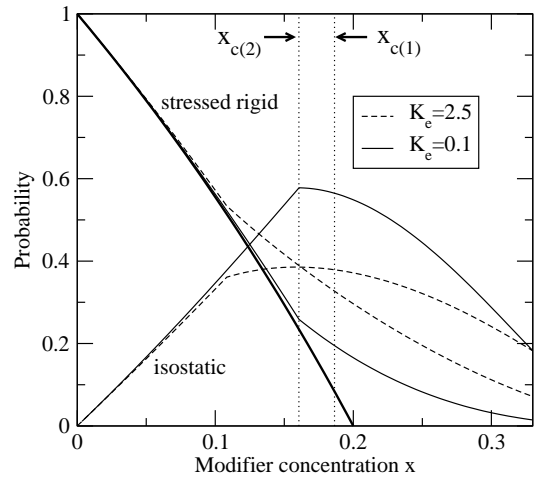


FIG. 3: Probability of finding stressed rigid and isostatically rigid clusters with respect to the modifier concentration  $x$  for two different equilibrium constants:  $K_e = 0.1$  (solid line) and  $K_e = 2.5$  (broken line). Note that the stressed rigid cluster probability extrapolates to  $x_c = 0.20$  in the MF description (bold line). The dotted vertical lines serve to define the two transitions and the intermediate phase for  $K_e = 0.1$ . Here  $\eta = 0.33$ .

value of  $K_e$  leads to the growth of even more flexible units ( $Q^2$ 's,  $n_c = 2.0$  per atom) to the expense of  $Q^3$ 's, and will produce a stress transition at lower  $x$  (broken line, Fig. 3). Indeed, increasing  $K_e$  at fixed  $x$  decreases the network mean coordination number and favours flexible  $Q^4 - Q^2$  instead of isostatically rigid  $Q^4 - Q^3$  bondings. As a result, with growing concentration  $x$ , the network will lose stress earlier and will display a lower isostaticity in the IP. Thus  $x_{c(2)}$  is shifted to lower  $x$ .

The constraint-related free energy is now considered, following the approach initially reported by Naumis [26]. The free energy of the system is given by:

$$\mathcal{F}_{(2)}(x, K_e) = -f^{(2)} + k_B T \sum_{k,j} p_{kj}^{(2)} \ln p_{kj}^{(2)} \quad (4)$$

where  $-f^{(2)}$  is the stress energy equal to the number of redundant constraints, i.e. additional constraints that cannot be balanced by the degrees of freedom, and which vanish for  $x > x_{c(1)}$ . Figure 4 shows that the stress transition at  $x = x_{c(2)}$  is first order for any  $K_e$ . However, with respect to the mean-field case (bold solid line) where  $x_{c(1)} = x_{c(2)}$ , the jump of the first derivative  $\partial \mathcal{F}_{(2)}(x, K_e) / \partial x$  at  $x = x_{c(2)}$  decreases with growing  $K_e$ . In the MF case, this jump is equal to 75.22, whereas it is only 45.30 for  $K_e = 2.5$ . This suggests that the transition broadens when the equilibrium (1) displaces to the right side, leading to a  $Q^2$ -rich glass. On the other hand, the change in character with  $K_e$  of the rigidity transition is weak and second order. Finally, some chemical self-organization of the network is allowed through

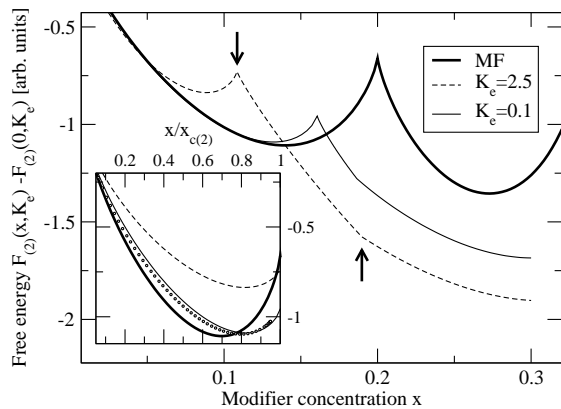


FIG. 4: Free energy  $\mathcal{F}_{(2)}(x, K_e) - \mathcal{F}_{(2)}(0, K_e)$  of the system as a function of the modifier concentration  $x$  in the mean-field case (bold solid line), and for two different equilibrium constants:  $K_e = 0.1$  (solid, line) and  $K_e = 2.5$  (broken line), both for  $\eta = 0.33$ . The arrows indicate the stress and rigidity transition for  $K_e = 2.5$ . The insert shows the same quantity with  $x$  rescaled to its stress transition composition  $x_{c(2)}$ , together with the free energy (dots) minimized by  $K_e$ . In all,  $k_B T = 1$ .

an adaptative speciation. As stress costs energy, it is natural to imagine that the glass network will try to self-organize in the stressed rigid phase to decrease the energy by rewiring and reset some weaker bonds such as the ionic M-X ones that will lead to a  $Q^n$  specie recombination. In the present description, this means that at a given concentration  $x < x_{c(2)}$ , the minimization of the free energy can be accomplished with respect to  $K_e$ . The equilibrium constant  $K_e$  minimizing  $\mathcal{F}(x, K_e)$  provides then an estimation of the speciation *via equ.* (2) and the probability of stressed rigid clusters. This leads to a stress transition at  $x = x_{c(2)} = 0.168$  and a free energy (dots in the insert of Fig. 4) that is very close to the  $K_e = 0.1$  speciation model and to sodium silicates [20].

In summary, with decreasing modifier concentration  $x$  there are different ways for a flexible system to self-organize in order to avoid stress, either by nucleating weak stress in small rings (EST), or by producing more flexible local structures ( $Q^2$ 's) that balance the addition of new constraints arising from the decrease of the modifier content. Both delay the onset of stressed rigidity. As a conclusion, we provide a prediction of the IP for sodium selenosilicates (M=Na, X=Se) that have an EST fraction of  $\eta = 0.50$  in the base network former  $SiSe_2$  [27] and an equilibrium constant  $K_e = 0.15$  [?]. According to the present approach, one therefore expects a stress transition at  $x_{c(2)} = 0.113$ , a rigidity transition at  $x_{c(1)} = 0.182$  and a width for the Intermediate Phase of about  $\Delta x = 0.069$ . Larger structural correlations will probably refine this picture and are under consideration.

It is a pleasure to acknowledge ongoing discussions with P. Boolchand, B. Goodman, M. Malki and P. Si-

mon. LPTMC is Unité Mixte de Recherche du Centre National de la Recherche Scientifique (CNRS) n. 7600.

- 
- [1] J.L. Lagrange, *Mécanique Analytique* (Paris) 1788; J.C. Maxwell, *Phil. Mag.*, **27** (1864) 294.
  - [2] *Rigidity theory and applications*, M.F. Thorpe, P.M. Duxbury Eds. (Plenum Press/ Kluwer), New York 1999.
  - [3] M.F. Thorpe, *J. Non-Cryst. Solids* **57**, 355 (1983); H. He, M.F. Thorpe, *Phys. Rev. Lett.* **54**, 2107 (1985).
  - [4] J.C. Phillips, *J. Non-Cryst. Solids* **34**, 153 (1979). For an r-folded atom, the number of bond-stretching and bond-bending mechanical constraints is  $n_c = 5r/2 - 3$ .
  - [5] P. Boolchand, G. Lucovsky, J.C. Phillips, M.F. Thorpe, *Phil. Mag.* **85**, 3823 (2005); D. Selvenathan, W. Bresser, P. Boolchand, *Phys. Rev.* **B61**, 15061 (2000); D.G. Georgiev, P. Boolchand, M. Micoulaut, *Phys. Rev.* **B62**, 9228 (2000); P. Boolchand, D.G. Georgiev, B. Goodman, *J. Optoelectr. Adv. Mater.*, **3**, 703 (2001).
  - [6] S. Chakravarty, D.G. Georgiev, P. Boolchand, M. Micoulaut, *J. Phys. Cond. Matt.* **17**, L7 (2005).
  - [7] F. Wang, S. Mamedov, P. Boolchand, B. Goodman, M. Chandrasekhar, *Phys. Rev.* **B71**, 174201 (2005); C. Popov, S. Boycheva, P. petkov, Y. Nedeva, B. Monchev, S. Parvanov, *Thin. Sol. Films* **496**, 718 (2006).
  - [8] J. Gump, I. Finkler, H. Xia, R. Sooryakumar, W.J. Bresser and P. Boolchand, *Phys. Rev. Lett.* **92**, 245501 (2004)
  - [9] M.F. Thorpe, D.J. Jacobs, M.V. Chubynsky, J.C. Phillips, *J. Non-Cryst. Solids* **266-269**, 859 (2000)
  - [10] M. Micoulaut, J.C. Phillips, *Phys. Rev.* **B67**, 104204 (2003)
  - [11] A.J. Rader, B. Hespeneide, L. Kuhn, M.F. Thorpe, *Proc. Natl. Acad. Sci.* **99**, 3540 (2002)
  - [12] J.C. Phillips, *Phys. Rev. Lett.* **88**, 216401 (2002)
  - [13] R. Monasson, R. Zecchina, S. Kirkpatrick, B. Selman, L. Troyansky, *Nature*, **400** (1999) 133.
  - [14] J. Barré, A.R. Bishop, T. Lookman, A. Saxena, *Phys. Rev. Lett.* **94**, 208701 (2005).
  - [15] A. Huerta, G.G. Naumis, *Phys. Rev. Lett.* **90**, 145701 (2003).
  - [16] M.V. Chubynsky, M.A. Brière, N. Mousseau, cond-mat/0602412.
  - [17] Y. Vaills, T. Qu, M. Micoulaut, F. Chaimbault, P. Boolchand, *J. Phys. Cond. Matt.*, **17**, 4889 (2005).
  - [18] X. Feng, W. Bresser, P. Boolchand, *Phys. Rev. Lett.* **78**, 4422 (1997).
  - [19] M. Zhang, P. Boolchand, *Science* **266**, 1355 (1994).
  - [20] B.O. Mysen, *Eur J. Mineral.* **15**, 781 (2003).
  - [21] J.F. Stebbins, *Nature* **330**, 465 (1987).
  - [22] A. Pradel, G. Taillades, M. Ribes, H. Eckert, *J. Non-Cryst. Solids* **188**, 75 (1995); H. Eckert, A. Pradel, J.H. Kennedy, M. Ribes *J. Non-Cryst. Solids* **113**, 287 (1989).
  - [23] P.J. Bray, S.A. Feller, G.E. Jellison, and Y.H. Yun, *J. Non-Cryst. Solids* **38-39**, 93 (1980).
  - [24] J.F. Stebbins, *J. Non-Cryst. Solids* **106**, 359 (1988)
  - [25] C.M. Schramm, B.H. DeJong, V.F. Parziale, *J. Am. Chem. Soc.* **106**, 4396 (1984).
  - [26] G.G. Naumis, *Phys. Rev.* **B61**, R9205 (2000).
  - [27] M. Tenhover, M.A. Hazle, R.K. Grasselli, *Phys. Rev. Lett.* **51**, 404 (1983)